Etienne Berthier
14 av Ed Belin
31400 Toulouse
etienne.berthier@legos.obs-mip.fr

13 March 2018

Dear editor,

Please, find enclosed a revised version of our manuscript (MS) entitled “Brief communication: Unabated wastage of the Juneau and Stikine icefields (southeast Alaska) in the early 21st century”. To facilitate your assessment, we uploaded a track-change version of the revised MS.

We thank the two reviewers for their positive evaluation of our study. Find below a copy of their comments and, in bold/blue, a point-by-point response to them. The revised text is provided in italics.

In addition to the reviewer’s comments, we also corrected Figure 2b, where Melkonian et al. 2014 was replaced by Melkonian et al. 2016. We thank F. Brun for spotting this error.

We hope that these corrections/clarifications make our paper now suitable for publication in The Cryosphere.

Yours sincerely,

Etienne Berthier and co-authors

Reply to reviewer#1, Robert McNabb

Summary

In this manuscript, the authors have investigated the source of an apparent slowdown in the mass loss of the Juneau and Stikine Icefields, Alaska, by comparing multiple studies and data sources, re-processing the data used in a consistent fashion. They contend that the source of the signal seen is due to the use of the SRTM C-band DEM by two studies, Melkonian and others (2014) and Melkonian and others (2016), and not due to an actual slowing in the rate of mass loss for the glaciers studied. The authors show that the unknown penetration depth of the SRTM C-Band radar signal into snow and ice causes a significant underestimation of elevation lowering, and therefore volume and mass losses for the two icefields. I think that the methods described in the manuscript are sound, and the results well-presented and reasonable. As such, I have only minor comments on the manuscript, otherwise recommending that it be accepted for publication in The Cryosphere.

Minor comments

l. 85: Does this mean less than 0.5% of the icefield, after processing the DEMs and masking clouds, blunders, etc.?

> **Reply: The sentence has been clarified and now reads "***Images in which valid elevation data covered less than 0.5% of the icefield areas were excluded, ...***"**

l. 88: Why the RGI v5.0, rather than v6.0?

> **Reply: At the time of our study, RGI v6.0 was not published. Anyway, outlines are unchanged for the study area between RGI 5.0 and 6.0.**

l. 132: Make sure the minus sign is on the same line as the number.

> **Reply: Thanks, we will be careful while proof-reading the article.**

l. 134: It's not clear to me what you mean by "statistically different for the JIF" - can you elaborate on this?

> **Reply: We improved the text by adding "***, i.e. the JIF mass balances do not overlap given the error bars.***"**

l. 181: "for both datatsets"

> **Reply: Corrected here (and elsewhere in the MS).**

Table 1: It might be good to plot these data, perhaps as a supplemental figure, to ease the comparison of the values and mesh with your opening discussion statement.

> **Reply: Supplementary Figure S2 added and referred to in the opening discussion statement**

l. 271: I'm not sure what this sentence is meant to be saying - it seems like you stopped mid-thought while writing it.

> **Reply: Sorry of the typo. "is linked to the" has now been removed.**

Reply to reviewer#2, Mauri Pelto

Berthier et al (2017) provide a detailed update of the mass balance record of two large icefields in southeast Alaska and an updated method of determination. The geodetic mass balance based on ASTER images is a significant improvement over previous combined analysis use ASTER and SRTM. Particularly on the Juneau Icefield the record is validated against both field mass balance observations and laser altimetry. The results is a robust record. The paper also provides a detailed review of how the SRTM data proved unreliable due to variable C-band penetration of snow and firn. This is an important and concise update in approach that should be used to reassess other geodetic mass balance records that used best practices at the time, but may have this same correctable bias.

Specific Comments: The two different line numbers result from two different line numbering versions of the paper. Not sure which the authors will utilize.

40 or 45: Indicate that Lemon Creek Glacier is a WGMS reference glacier. Also separately note that the record to reflect that the Lemon Creek Glacier record from 2000-2016 is -0.56 m w.e. a-1 (WGMS, 2017).

> **Reply: We now indicate in the introduction that Lemon Creek is a WGMS reference glacier. The 2000-2016 mass balance of this glacier is also compared to our ASTER-based estimates at the end of the Results section.**

65: Field observations of the ELA and mass balance do not support a slow down.

> **Reply: Statement added in the introduction. "***Field observations of the equilibrium line altitude and mass balance do not support a slow down (WGMS, 2017).***"**

108 or 118: Taku Glacier (southern outlet of JIF)"

> **Reply: text corrected.**

110 or 120: Should be reported that the most extensive thinning of the lower reach of JI glaciers is associated with lacustrine calving retreats on Field, Gilkey, Llewellyn, Meade, Mendenhall, and Tulsequah glacier (Pelto, 2017), which also notes that every outlet glacier retreated significantly except Taku Glacier. This supports the line 48 statement as well. On Stikine Icefield lacustrine and tidewater calving retreat during the study period occurred on Baird, Dawes, Great, Sawyer, South Sawyer, Speel and Wright Glacier.

> **Reply: We believe that this is beyond the scope of the paper. Our goal is not to compare and try to explain the variability in individual glacier mass balances. Together with the reference noted by the reviewer, the issue has been addressed in detail in Larsen et al., GRL, 2015. The text is thus unaltered.**

146 or 156: Any thoughts on why the difference? This is in the terminus region for many glaciers including lake formation zone.

> **Reply: We have no straightforward explanation for these differences. No such difference is observed for the terminus area of the Stikine icefield. We further note that the fraction of the glacier area covered by these terminus regions are rather small so that they do not count much in the overall mass budget. However, we reckon that they are important for process understanding.**

181 or 195: Separately note that the mass balance of Taku Glacier from 2000-2016 is -0.08 m w.e. a-1 (WGMS, 2017).

Reply: Text has been modified to include the 2000-2016 Taku mass balance.

Consider the value of citing Pelto et al (2008) pointed out the mass balance transition."Surface mass balance was positive from 1946-1988 +0.42 ma-1. This led to glacier thickening. From 1988-2006 an important change has occurred and annual balance has been -0.14 ma-1, and the glacier thickness has ceased increasing along Profile IV."

Reply: This reference was added in the introduction. "*This statement is also valid for Taku Glacier, for which the mass balance was positive (+0.42 m w.e. a-1) from 1946-1988 and negative (-0.14 m w.e. a-1) during 1988-2006 (Pelto et al., 2008).”*

Table 1: Should add column for the field observed mass balance for Taku Glacier and Lemon Creek Glacier.

Reply: As glaciological mass balance are available for only two of the compared glaciers we prefer to mention them in the discussion text, not in the table.

242 or 264: The linear correction used by Larsen et al (2007) would depend on the season of comparison.

Reply: We are unsure what the referee means here. Our text is thus currently unaltered.

249 or 271: remove "is linked to the"

Reply: Removed. Thanks for spotting this.

254 or 276: Winter balance observations on Taku Glacier support this seasonal amplitude.

Reply: We modified the text, stating: *“Assuming a seasonal amplitude as large as 10 m (a value in agreement with field measurements of the Juneau Icefield Mass Balance Program, Pelto et al., 2013), the slope of the regression”*

262 or 286: which is in agreement with the altimetry and field based assessments on a smaller sample of these glaciers.

Reply: Statement added in the first sentence of the introduction.

275 or 301: Is it worth elaborating for one sentence on the Tandem X issues? Also are the issues much reduced in summer for Tandem X?

Reply: We simply added *“, except if water is present in the snow and firn upper layers at the time of acquisition of the radar images”*

Brief communication: Unabated wastage of the Juneau and Stikine icefields (southeast Alaska) in the early 21st century

Etienne BERTHIER[1], Christopher LARSEN[2], William J. Durkin[3], Michael J. Willis[4], Matthew E. Pritchard[3]

[1] LEGOS, Université de Toulouse, CNES, CNRS, IRD, UPS, F-31400 Toulouse, France
[2] Geophysical Institute, University of Alaska Fairbanks, Fairbanks, Alaska, USA
[3] Earth and Atmospheric Sciences Department, Cornell University, Ithaca, New York, USA
[4] Cooperative Institute for Research in Environmental Sciences (CIRES), University of Colorado, Boulder, CO, USA

Correspondence to: Etienne Berthier (etienne.berthier@legos.obs-mip.fr)

Abstract. The large Juneau and Stikine icefields (Alaska, JIF and SIF) lost mass rapidly in the second part of the 20th century. Laser altimetry, gravimetry and sparse field measurements suggest continuing mass loss in the early 21st century. However, two recent studies based on time series of SRTM and ASTER digital elevation models (DEMs) indicate a slowdown in mass loss after 2000. Here, the ASTER-based geodetic mass balance is recalculated, carefully avoiding the use of the SRTM DEM because of the unknown penetration depth of the C-Band radar signal. We find strongly negative mass balances from 2000 to 2016 (-0.68±0.15 m w.e. a^{-1} for JIF and -0.83±0.12 m w.e. a^{-1} for SIF), in agreement with laser altimetry, confirming that mass losses are continuing at unabated rates for both icefields. The SRTM DEM should be avoided or used very cautiously to estimate glacier volume change, especially in the North Hemisphere and over timescales of less than ~20 yrs.

1 Introduction

The Juneau Icefield (JIF) and Stikine Icefield (SIF) are among the largest and southernmost icefields in Alaska. The JIF covers about 3800 km² and the SIF close to 6000 km² at the border between southeast Alaska and Canada (Kienholz et al., 2015). Together they account for roughly 10% of the total glacierized area in Alaska. Both icefields experienced rapid mass loss in the second part of the 20th century (Arendt et al., 2002; Berthier et al., 2010; Larsen et al., 2007). Spaceborne gravimetry and laser altimetry data suggest continuing rapid mass loss in southeast Alaska between 2003 and 2009 (Arendt et al., 2013).

For the JIF, Larsen et al. (2007) found a negative mass balance of -0.62 m w.e. a^{-1} for a time interval starting in 1948/1982/1987 (depending on the map dates) and ending in 2000, the date of acquisition of the shuttle radar topographic mission (SRTM) digital elevation model (DEM). Berthier et al. (2010) found a slightly less negative multi-decadal mass balance (-0.53 ± 0.15 m w.e. a^{-1}) from the same starting dates as Larsen et al. (2007) to a final DEM acquired in 2007. Repeat airborne laser altimetry are available for nine glaciers of the JIF (Larsen et al., 2015) with a first survey performed in 1993 (2 glaciers), 1999 (1 glacier) and 2007 (6 glaciers). The last

survey used in Larsen et al. (2015) was flown in 2012 for all glaciers. During these varying time intervals, nine glaciers experienced strongly negative mass balances (between -0.51 and -1.14 m w.e. a^{-1}) while Taku Glacier, which alone accounts for one fifth of the JIF area, experienced a slightly positive mass balance (+0.13 m w.e. a^{-1}). Further, the glaciological measurements performed on Lemon Creek Glacier (11.8 km² in 1998, a world glacier monitoring service (WGMS) reference glacier) suggest accelerated mass loss since the mid-eighties: the glacier-wide mass balance declined from -0.30 m w.e. a^{-1} during 1953-1985 to -0.60 m w.e. a^{-1} during 1986-2011 (Pelto et al., 2013). This statement is also valid for Taku Glacier, for which the mass balance was positive (+0.42 m w.e. a^{-1}) from 1946 to 1988 and negative (-0.14 m w.e. a^{-1}) from 1988 to 2006 (Pelto et al., 2008). A modelling study also found a negative mass balance for the entire JIF (-0.33 m w.e. a^{-1}) for 1971-2010 (Ziemen et al., 2016). Their 40-year mass balance is a result of glacier mass stability until 1996 and rapid mass loss afterwards. Taken together, all these studies point toward rapid mass loss of the JIF and accelerated wastage during the last ~20 years. Conversely, a study based on the SRTM DEM and Advanced Spaceborne Thermal Emission and Reflection Radiometer (ASTER) multi-temporal DEMs found a JIF mass balance only moderately negative at -0.13 ± 0.12 m w.e. a^{-1} from 2000 to 2009/2013 (Melkonian et al., 2014).

Supprimé: -
Supprimé: during
Supprimé:
Mis en forme : Exposant
Supprimé: -
Mis en forme : Exposant
Supprimé:

Only a few estimates of mass change are available on the larger and more remote SIF. Three of its glaciers were surveyed with airborne laser altimetry from 1996 to 2013 and all experienced rapid mass loss. The glacier-wide mass balances were -0.71, -0.98 and -1.19 m w.e. a^{-1} for, respectively, Baird, Le Conte and Triumph glaciers. Based on DEM differencing over several decades, Larsen et al. (2007) and Berthier et al. (2010) found SIF-wide mass balance of, respectively, -1.48 and -0.76 ± 0.12 m w.e. a^{-1}. A recent estimate based on the SRTM and ASTER DEMs suggest a less negative icefield-wide mass balance of -0.57 ± 0.18 m w.e. a^{-1} from 2000 to 2014 (Melkonian et al., 2016).

If correct, Melkonian et al. (2014, 2016)'s estimates would imply a considerable slowdown of the mass loss of the Juneau and, to a smaller extent, Stikine icefields during the first decade of the 21st century. However, no clear trend in climate such as cooling or increased precipitation was found during this period to explain such a slow down (Melkonian et al., 2014; Ziemen et al., 2016). Field observations of the equilibrium line altitudes and surface mass balances do not support a slow down (WGMS, 2017). Further, Melkonian et al. (2014, 2016)'s estimates used as starting elevation measurement the C-Band SRTM DEM acquired in February 2000, the core of winter in Alaska. The C-Band radar signal is known to penetrate into the cold winter snow and firn such that SRTM maps a surface below the real glacier surface which can bias the elevation change measurements (e.g., Berthier et al., 2006; Rignot et al., 2001). Melkonian et al. (2014, 2016) accounted for this penetration by subtracting the simultaneous C-Band and X-Band SRTM DEM, assuming no penetration of the X-Band DEM (Gardelle et al., 2012), the best available correction at the time of their study. However, this strategy is not appropriate given that the X-band penetration depth has recently been recognized to reach several meters (e.g., Dehecq et al., 2016; Round et al., 2017). In this context, the goal of this brief communication is to

recalculate the early 21st century geodetic mass balances of the Juneau and Stikine icefields using multi-temporal ASTER DEMs, carefully excluding the SRTM DEM to avoid a likely penetration bias.

2 Data, methods and uncertainties

The data and methodology applied to the JIF and SIF were identical to the ones used in a recent study deriving region-wide glacier mass balance in High Mountain Asia (Brun et al., 2017). The reader is thus referred to the latter study for details. Only the main processing steps are briefly presented here.

ASTER DEMs were calculated using the open-source Ames Stereo Pipeline (ASP) (Shean et al., 2016) from 3N (nadir) and 3B (backward) images acquired between 2000 and 2016. All images with cloud coverage lower than 80% were selected, resulting in 153 stereo pairs for the JIF and 368 stereo pairs for the SIF. Images in which valid elevation data covered less than 0.5% of the icefield areas were excluded, reducing the number of stereo pairs to 114 for the JIF and 284 for the SIF. Planimetric and altimetric offsets of each ASTER DEM were corrected using the SRTM DEM as a reference. Offsets were determined on stable terrain, masking out glacierized areas using the Randolph Glacier Inventory v5.0 (Pfeffer et al., 2014). The RGI v5.0 glacier outlines for both the JIF and SIF were mapped using imagery from August of 2004 and 2005 (Kienholz et al., 2015).

Supprimé: intersecteding

For the JIF only, we also downloaded directly the ASTER DEMs available online from the LPDAAC website (called 14DMO) because they were used in Melkonian et al. (2014, 2016). The goal is to test the sensitivity of the JIF-wide mass balance to the ASTER DEM generation software. 3D coregistration of the 14DMO DEMs was performed using the same steps as the ASP DEMs. Unlike the ASP DEMs, the 14DMO DEMs contain no data gaps, as they are filled by interpolation.

From the time series of 3D-coregistered ASTER DEMs, the rate of elevation changes (*dh/dt* in the following) was extracted for each pixel of our study domain in two steps (Berthier et al., 2016). The SRTM DEM was excluded when extracting the final *dh/dt*. *dh/dt* were calculated for the entire period (from 2000 to 2016) and also for different sub-periods for the sake of comparability to published mass balance estimates.

For both icefields and in each 50-m altitude interval, *dh/dt* lying outside of ±3 normalized median absolute deviations (NMAD) were considered as outliers. We further excluded all *dh/dt* measurements for which the error in the linear fit is larger than 2 m a^{-1}. The total volume change rate was calculated as the integral of the mean *dh/dt* over the area altitude distribution. The icefield-wide mass balance was obtained using a volume-to-mass conversion factor of 850 ± 60 kg m^{-3} (Huss, 2013). The same procedure was followed to compute the glacier-wide mass balances of selected individual glaciers for which mass balances were estimated from repeat laser altimetry surveys (Larsen et al., 2015).

Uncertainties for *dh/dt* were computed using the tile method as in Berthier et al. (2016). Splitting the off-glacier terrain in 4 by 4 tiles, we found uncertainties of 0.03 m a^{-1} for JIF and 0.04 m a^{-1} for SIF from 2000 to 2016. When data gaps occurred in the *dh/dt* map, we conservatively multiplied these uncertainties by a factor of five.

3 Results

Rate of elevation changes for the two icefields from 2000 to 2016 are mapped in Figure 1. Most glaciers thinned rapidly in their lower parts and experienced limited elevation change in their upper reaches. Thinning rates as negative as 9 m a^{-1} are observed. Taku Glacier (southern outlet of the JIF) is an exception with thickening of up to 4 m a^{-1} at its glacier front.

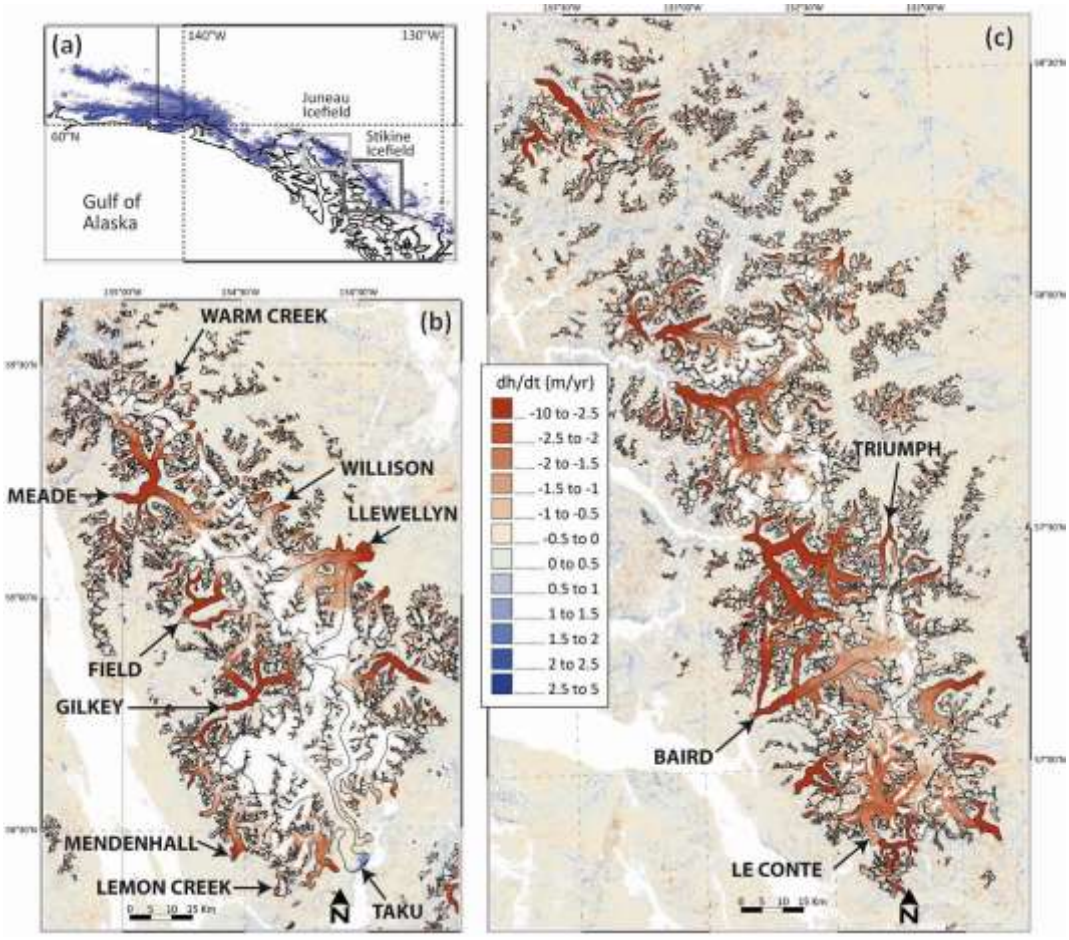

Figure 1: Rate of elevation changes for the Juneau and Stikine icefields from 2000 to 2016. (a) Location of the two icefields in southeast Alaska. Rate of elevation changes (*dh/dt*) for the JIF (b) and (c) for the SIF. Glacier outlines are from RGI v5.0. Glaciers surveyed by airborne laser altimetry are labelled. The horizontal scale and the color code are the same for the two maps. Areas in white correspond to data gaps.

The 2000-2016 mass balances are clearly negative for both icefields at -0.68±0.15 m w.e. a^{-1} for JIF (59% coverage with valid data) and -0.83±0.12 m w.e. a^{-1} for SIF (81% coverage with valid data). If we apply the linear

regression analysis to a subset of the ASTER DEMs to match the time periods studied by Melkonian et al. (2014, 2016), the icefield-wide mass balances remain mostly unchanged: -0.64±0.14 m w.e. a^{-1} for JIF from 2000 to 2013, 44% coverage with valid data; -0.78±0.17 m w.e. a^{-1} for SIF from 2000 to 2014, 55% coverage with valid data. Our values are 0.51±0.18 m w.e. a^{-1} (JIF) and 0.21±0.25 m w.e. a^{-1} (SIF) more negative than in Melkonian et al. (2014, 2016) and statistically different for the JIF, i.e. the JIF mass balances do not overlap given the error bars.

The coverage with valid *dh/dt* data drops rapidly for both icefields when shorter time periods are considered. For example, the percentage of valid data is reduced to 8% (respectively 25%) only on the JIF when the 2000-2008 (respectively 2008-2016) period is analyzed. Thus, the ASTER multi-temporal analysis is not appropriate to measure mass balance over periods shorter than 10 years for these two Alaskan icefields. This is due to the presence of many cloudy images and, for cloud-free scenes, to a large percentage of data gaps in individual ASTER DEMs over the accumulation areas of the icefields, a direct result of the limited contrast in the ASTER stereo-images over textureless snow fields.

In Figure 2, *dh/dt* are plotted as a function of altitude and compared to the values in Melkonian et al. (2014, 2016). To enable a more direct comparison, we applied the same criteria to average their *dh/dt* in 50-m altitude bands and exclude outliers. We also considered the same periods, from 2000 to 2013 for the JIF and from 2000 to 2014 for the SIF. In the case of the SIF (Figure 2b), we also added the *dh/dt* obtained by applying our method to the 14DMO DEMs.

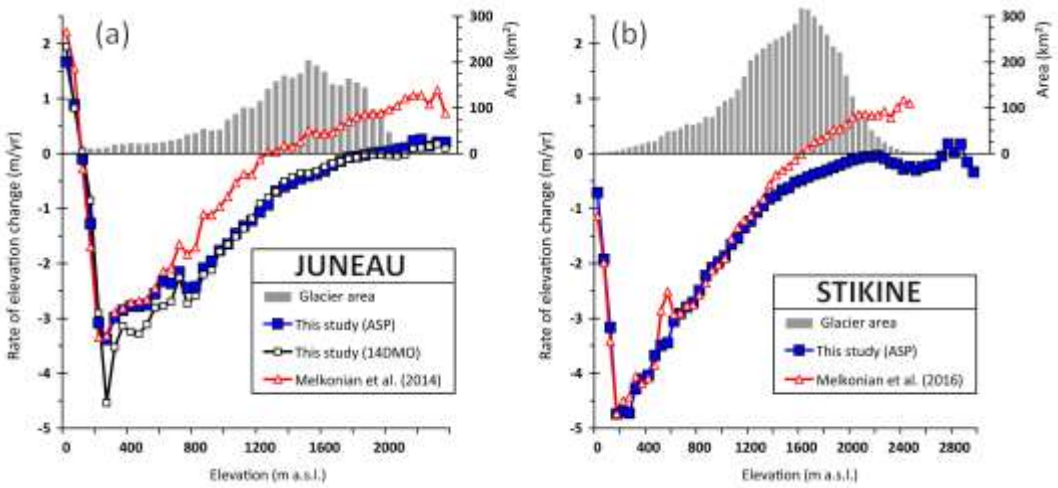

Figure 2: Rates of elevation change vs. elevation for the JIF from 2000 to 2013 (a) and for the SIF from 2000 to 2014 (b). Results from this study are compared to the *dh/dt* values obtained in two earlier studies using a similar method (Melkonian et al., 2014, 2016). The grey histograms show the area-altitude distribution.

For the JIF, an excellent agreement is found between the *dh/dt* values obtained in this study using the ASP and 14DMO DEMs, except maybe between 250 and 600 m a.s.l. (5% of the icefield area) where the thinning rates are about 0.5 m a^{-1} more negative using the 14DMO DEMs. The area-weighted mean absolute difference between these two curves (ASP and 14DMO) is 0.09 m a^{-1}. The Melkonian et al. (2014) *dh/dt* generally agree with ours below 600 m a.s.l. Above this elevation, their values are systematically more positive. The difference reaches 0.7 m a^{-1} at 800 m a.s.l. and then remains more or less stable, around 0.7-0.9 m a^{-1}. Melkonian et al. (2014) data suggests thickening of the areas above 1350 m a.s.l. where 62% of the JIF area is located.

For SIF, a good agreement is found between ours and Melkonian et al. (2016)'s *dh/dt* below an elevation of 1300 m a.s.l. Above 1300 m the two curves diverge. Our *dh/dt* are becoming less negative until 2100 m a.s.l. where they become indistinguishable from 0 m a^{-1} up to the SIF highest elevation band. Conversely, in the Melkonian et al. (2016) dataset, *dh/dt* increases rapidly, crossing 0 m a^{-1} at ~1650 m a.s.l., finally arriving at a thickening rate of > 0.7 m a^{-1} above 2000 m a.s.l. Thus the difference in SIF-wide mass balance between the two datasets is due to difference in *dh/dt* above 1300 m a.s.l., where 66% of the SIF icefield area is found.

Comparison of our *dh/dt* estimates to the ones derived from repeat laser altimetry data is not straightforward because the survey periods differ. For example, for the JIF, six out of nine glaciers were sampled for the first time in 2007. In most cases, it would be technically possible to use a temporal subset of the ASTER DEMs to match the time period of altimetry surveys but, as said above, this would be at the cost of the coverage in our *dh/dt* maps and would lead to much more uncertain mass balance estimates. Consequently, we preferred to extract *dh/dt* and the individual glacier mass balance for the longest available time period in the ASTER series (from 2000 to 2016) in order to maximize coverage and thus minimize uncertainties. The pattern of *dh/dt* with altitude for individual glaciers is in broad agreement between laser altimetry and our ASTER-based results (Supplementary Figure S1). Importantly, for both datasets, no clear thickening was observed in the accumulation areas of glaciers. When individual elevation bins of 50 m are considered, averaged differences between *dh/dt* from laser altimetry and the ASTER DEMs are typically 0.2 to 0.3 m a^{-1} for individual glaciers. This level of error is similar to the one found previously for the ASTER method in the Mont-Blanc area (Berthier et al., 2016). Glacier-wide mass balances for individual glaciers match well (Table 1, Supplementary Figure S2).

The mean mass balance of these 12 glaciers is nearly the same (-0.73 and -0.74 m w.e. a^{-1}) using the two techniques. The standard deviation of the mass balance difference is 0.18 m w.e. a^{-1} (n=12). For 60 individual glaciers larger than 2 km² in High Mountain Asia, Brun et al. (2017) also found a standard deviation of 0.17 m w.e. a^{-1} between the ASTER-based and published glacier-wide mass balance estimates. In the very different geographic context of large maritime glaciers of southeast Alaska, we confirm here their uncertainty estimate for individual glaciers in High Mountain Asia.

Our results are also in good agreement with field (glaciological) measurements on Taku and Lemon Creek glaciers. For Taku Glacier, found the mass balance was -0.01 m w.e. a^{-1} between September 2000 and September 2011 (Pelto et al., 2013) and -0.08 m w.e. a^{-1} between September 2000 and September 2016 (WGMS, 2017). We derived a very similar glacier-wide mass balance (-0.01 ± 0.16 m w.e. a^{-1}) from ASTER DEMs acquired between 2000 and 2016. Conversely, Melkonian et al. (2014)'s mass balance for Taku Glacier was strongly positive at +0.44 ± 0.15 m w.e. a^{-1}. The 2000-2016 mass balance for Lemon Creek Glacier is -0.56 m w.e. a^{-1} (WGMS, 2017) while our ASTER-based mass balance is just slightly more negative at -0.78 ± 0.14 m w.e. a^{-1}.

Supprimé: G
Supprimé: Pelto et al. (2013)
Supprimé: a
Supprimé: of
Supprimé: the
Supprimé: same
Mis en forme : Exposant

Table 1. Glacier-wide mass balances (B_a) of 12 individual glaciers of the JIF and SIF derived from airborne laser altimetry for different periods (Larsen et al., 2015) and calculated in this study using ASTER DEMs from 2000 to 2016.

Icefield/Glacier	Area km²	Laser period	B_a Laser m w.e. a^{-1} (Larsen et al., 2015)	B_a ASTER m w.e. a^{-1} (this study)
Juneau	**3398**			**-0.68**
Field	187	2007-2012	-0.94	-0.93
Gilkey	223	2007-2012	-0.75	-0.99
Lemon Creek	9	1993-2012	-0.91	-0.78
Llewellyn	435	2007-2012	-0.61	-0.70
Meade	446	2007-2012	-1.03	-0.88
Mendenhall	106	1999-2012	-0.57	-0.73
Taku	711	1993-2012	0.13	-0.01
Warm Creek	39	2007-2012	-0.67	-0.71
Willison	79	2007-2012	-0.51	-0.69
Sum/Mean 9 glaciers	**2234**		**-0.65**	**-0.71**
Stikine	**5805**			**-0.83**
LeConte	56	1996-2013	-0.98	-0.93
Baird	435	1996-2013	-0.71	-0.70
Triumph	356	1996-2013	-1.19	-0.86
Sum/Mean 3 glaciers	**847**		**-0.96**	**-0.83**
Mean all 12 Glaciers			**-0.73**	**-0.74**

4 Discussion

We find an excellent agreement between repeat laser altimetry survey and our multi-temporal analysis of ASTER DEMs both in term of mass balances and pattern of *dh/dt* with altitude for the JIF and SIF since 2000 (Supplementary Figure S1-S2). Our results also suggest that the limited number of glaciers sampled using laser

altimetry are representative of the icefields as a whole. This is rather expected for the JIF because 9 glaciers covering a large fraction of the icefield (66%) were monitored using airborne data but not straightforward for the SIF where only 3 glaciers, accounting for 15% of the total icefield area, were surveyed.

This agreement between our ASTER results and airborne laser altimetry, together with the fact that most studies point toward steady or accelerating mass losses in southeast Alaska (see introduction), suggest that the mass balance is overestimated in Melkonian et al. (2014, 2016). There are two main differences between Melkonian et al. (2014, 2016)'s method and ours that could explain these contending mass balances: (i) they did not generate the DEM themselves but directly download the 14DMO product from the LPDAAC website and (ii) they used the SRTM DEM as a starting elevation in their regression analysis to compute *dh/dt*.

To test the sensitivity of our results to the ASTER DEM generation software, we applied our processing chain (in particular, excluding the SRTM DEM to infer the final *dh/dt*) to the 14DMO DEMs. From 2000 to 2016, we found a JIF-wide mass balance of -0.67±0.27 m w.e. a^{-1}, in striking agreement with the value derived from ASP DEMs (-0.68±0.15 m w.e. a^{-1}). The pattern of *dh/dt* with elevation is also in excellent agreement (Figure 2a). Uncertainties are nearly doubled when applying our method to the 14DMO DEMs: this is explained by larger errors of *dh/dt* off glacier (0.06 m a^{-1} for 14DMO DEMs vs. 0.03 m a^{-1} for ASP DEMs) and a lower coverage of the JIF with valid *dh/dt* data (49% for 14DMO DEMs vs. 59% for ASP DEMs). The latter may appear counter-intuitive as the 14DMO DEMs are delivered with no data gaps. The larger percentage of data gaps in the final 14DMO *dh/dt* maps results from the higher noise level of the individual 14DMO DEMs and demonstrate the efficiency of our filters to exclude unreliable *dh/dt* values.

Thus, we conclude that a likely explanation why Melkonian et al. (2014, 2016) found too positive mass balance for the JIF and, to a lesser extent, for the SIF is associated with the SRTM DEM and in particular the penetration of the C-Band radar signal into cold winter snow and firn. This interpretation is further supported by the fact that *dh/dt* curves nicely agree in the ablation areas where SRTM penetration depth is negligible and diverge in the accumulation areas where the largest penetration depths are expected (Figure 2). As noted in the introduction, Melkonian et al. (2014, 2016) attempted to account for this by subtracting the C-Band and X-Band SRTM DEM, assuming no penetration of the X-Band DEM (Gardelle et al., 2012). However, studies have measured X-band penetration depth of several meters (e.g., Dehecq et al., 2016; Round et al., 2017). In the case of the SIF, Melkonian et al. (2016) assumed no penetration below 1000 m a.s.l. and 2 m for elevations above 1000 m. Aware of how uncertain this correction was, these authors also proposed (their supplementary material section 6.3 and, Table S4) a different correction with no penetration below 1000 m a.s.l. and a linear increase from 2 to 8 m from 1000-2500 m a.s.l. Using this alternative scenario, they found an icefield-wide mass balance of -0.85 m w.e. a^{-1}, in better agreement with our value of -0.78±0.17 m w.e. a^{-1} from 2000 to 2014. Their 2 to 8 m penetration depth is consistent with the penetration gradient we inferred here by subtracting the SRTM DEM from a reconstructed DEM, obtained by extrapolating *dh/dt* to the time of acquisition of the SRTM

as proposed in Wang and Kääb (2015). This is also consistent with a first-order estimate of the penetration depth inferred from the elevation difference between the SRTM DEM and laser altimetry profiles acquired in late August 1999 and May 2000 over Baird and Taku glaciers. However, the latter estimates should be considered with care considering the complexity to account for seasonal elevation changes, long term elevation changes and the difficulty to estimate the vertical offset between the two elevation datasets on ice-free terrain.

The fact that the positive bias in Melkonian et al. (2014, 2016) mass balances was larger for the JIF and than for the SIF suggests a larger SRTM penetration depth for the JIF. It indicates that the penetration is probably spatially variable (depending on the firn conditions in February 2000) such that a correction determined on a single icefield (or worse a single glacier) may not apply to neighbouring glacier areas.

Larsen et al. (2007) used the SRTM DEM as their final topography after applying a linear correction of SRTM with altitude (2.6 m per 1000 m elevation, with a -2.5 offset at 0 elevation) determined by comparing SRTM to August 2000 laser altimetry data. Such a correction would correspond to a maximum SRTM penetration of ~1.5-2 m above 1500 m a.s.l. much smaller than what we found here. Thus, the fact that SRTM penetration depth is larger than previously thought over southeast Alaska icefields may also explain why Larsen et al. (2007) found larger mass losses than Arendt et al. (2002) and Berthier et al. (2010) who both used only non-penetrating optical (Lidar or stereo-imagery) data.

An uneven seasonal distribution of the ASTER DEMs could bias the multi-annual mass balances derived using the ASTER method (Berthier et al., 2016). This is especially crucial in maritime environment such as southeast Alaska where large seasonal height variations are expected. As in the case of the Mont-Blanc area (Figure 6 in Berthier et al., 2016), we sampled an hypothetic seasonal cycle in surface elevation changes at the time of acquisition of all ASTER DEMs over the JIF and fitted a linear regression to the elevation change time series. Assuming a seasonal amplitude as large as 10 m (a value in agreement with field measurements of the Juneau Icefield Mass Balance Program, Pelto et al., 2013), the slope of the regression line is very close to 0 (-0.007 m a^{-1}) suggesting no seasonal bias in the dates of the ASTER DEMs. To confirm the lack of seasonal bias and because the majority of the ASTER images were acquired close to accumulation peak, we also calculated a mass balance for the JIF considering only the 61 ASTER DEMs acquired in March, April and May between 2000 and 2016. For this alternative mass balance estimate, the coverage with valid data is reduced to 38%. At -0.58±0.18 m w.e. a^{-1}, the JIF-wide mass balance is slightly less negative but not statistically different from the "all seasons" value (-0.68±0.15 m w.e. a^{-1}, 59% of valid data). The pattern of *dh/dt* with altitude is also very similar.

Supprimé: is linked to the

5 Conclusion

In this study, we show that the Juneau and Stikine icefields continued to lose mass rapidly from 2000 to 2016, which is in agreement with the altimetry and field based assessments on a smaller sample of these glaciers. The

mass balances from repeat airborne laser altimetry and multi-temporal ASTER DEMs are reconciled if the SRTM DEM is discarded when extracting the rate of elevation change on glaciers from the elevation time series. Multi-temporal analysis of DEMs derived from satellite optical stereo-imagery is thus a powerful method to estimate geodetic region-wide mass balances over time intervals of, typically, more than 10 years. The strength of the ASTER method lies in the fact that it is based on an homogeneous and continuous archive of imagery built since 2000 using the same sensor. Maintaining openly available medium- to high-resolution stereo capabilities should be a high priority among space agencies in the future.

Previously published mass balances for these Alaska icefields using SRTM and ASTER DEMs were likely biased positively because of the strong penetration of the C-Band and X-Band radar signal into the cold winter snow and firn in February, when the SRTM was flown. Accounting for this penetration by subtracting the C-Band and X-Band SRTM DEMs (as often done before) is not appropriate because the X-Band penetration depth can reach several meters, except if water is present in the snow and firn upper layers at the time of acquisition of the radar images. Caution should thus be used when deriving mass balance using SRTM and Tandem-X DEMs over time period of less than ~20 years. Comparing DEMs acquired at the same time of the year using the same radar wavelength (e.g., Neckel et al., 2013) is one promising strategy to limit the bias due to differential radar penetration.

Acknowledgements

We thank Robert McNabb and Mauri Pelto for their positive reviews of our study. We thank Fanny Brun for sharing her python codes and for spotting an error in one of our figures. We thank the Global Land Ice Measurement from Space (GLIMS) project that allowed the population of a vast archive of ASTER stereo images over glaciers. E.B. acknowledges support from the French Space Agency (CNES) and the Programme National de Télédétection Spatiale grant PNTS-2016-01.

Author contributions

E.B. designed the study, made the data analysis and lead the writing. C.L. provided the laser altimetry data. W.D., M.W. and M.P. provided unpublished results. All authors discussed the results and wrote the paper.

References

Arendt, A., Luthcke, S., Gardner, A., O'Neel, S., Hill, D., Moholdt, G. and Abdalati, W.: Analysis of a GRACE global mascon solution for Gulf of Alaska glaciers, Journal of Glaciology, 59(217), 913–924, doi:10.3189/2013JoG12J197, 2013.

Arendt, A. A., Echelmeyer, K. A., Harrison, W. D., Lingle, C. S. and Valentine, V. B.: Rapid wastage of Alaska glaciers and their contribution to rising sea level, Science, 297(5580), 382–386, 2002.

Berthier, E., Arnaud, Y., Vincent, C. and Remy, F.: Biases of SRTM in high-mountain areas: Implications for the monitoring of glacier volume changes, Geophysical Research Letters, 33(8), L08502, doi:10.1029/2006GL025862, 2006.

Berthier, E., Schiefer, E., Clarke, G. K. C., Menounos, B. and Rémy, F.: Contribution of Alaskan glaciers to sea-level rise derived from satellite imagery, Nat Geosci, 3(2), 92–95, doi:10.1038/ngeo737, 2010.

Berthier, E., Cabot, V., Vincent, C. and Six, D.: Decadal region-wide and glacier-wide mass balances derived from multi-temporal ASTER satellite digital elevation models. Validation over the Mont-Blanc area, Frontiers in Earth Science, 4, doi:10.3389/feart.2016.00063, 2016.

Brun, F., Berthier, E., Wagnon, P., Kaab, A. and Treichler, D.: A spatially resolved estimate of High Mountain Asia glacier mass balances from 2000 to 2016, Nature Geoscience, 10(9), 668–673, doi:10.1038/ngeo2999, 2017.

Dehecq, A., Millan, R., Berthier, E., Gourmelen, N. and Trouve, E.: Elevation changes inferred from TanDEM-X data over the Mont-Blanc area: Impact of the X-band interferometric bias, IEEE Journal of Selected Topics in Applied Earth Observations and Remote Sensing, 9(8), 3870–3882, doi:10.1109/JSTARS.2016.2581482, 2016.

Gardelle, J., Berthier, E. and Arnaud, Y.: Impact of resolution and radar penetration on glacier elevation changes computed from multi-temporal DEMs, Journal of Glaciology, 58(208), 419–422, 2012.

Huss, M.: Density assumptions for converting geodetic glacier volume change to mass change, The Cryosphere, 7(3), 877–887, doi:10.5194/tc-7-877-2013, 2013.

Kienholz, C., Herreid, S., Rich, J. L., Arendt, A. A., Hock, R. and Burgess, E. W.: Derivation and analysis of a complete modern-date glacier inventory for Alaska and northwest Canada, Journal of Glaciology, 61(227), 403–420, doi:10.3189/2015JoG14J230, 2015.

Larsen, C. F., Motyka, R. J., Arendt, A. A., Echelmeyer, K. A. and Geissler, P. E.: Glacier changes in southeast Alaska and northwest British Columbia and contribution to sea level rise, J Geophys Res-Earth, 112(F1), F01007, doi:10.1029/2006JF000586, 2007.

Larsen, C. F., Burgess, E., Arendt, A. A., O'Neel, S., Johnson, A. J. and Kienholz, C.: Surface melt dominates Alaska glacier mass balance, Geophysical Research Letters, 42(14), 5902–5908, doi:10.1002/2015GL064349, 2015.

Melkonian, A. K., Willis, M. J. and Pritchard, M. E.: Satellite-derived volume loss rates and glacier speeds for the Juneau Icefield, Alaska, Journal of Glaciology, 60(222), 743–760, doi:10.3189/2014JoG13J181, 2014.

Melkonian, A. K., Willis, M. J. and Pritchard, M. E.: Stikine Icefield Mass Loss between 2000 and 2013/2014, Frontiers in Earth Science, 4, 89, doi:10.3389/feart.2016.00089, 2016.

Neckel, N., Braun, A., Kropáček, J. and Hochschild, V.: Recent mass balance of the Purogangri Ice Cap, central Tibetan Plateau, by means of differential X-band SAR interferometry, The Cryosphere, 7(5), 1623–1633, doi:10.5194/tc-7-1623-2013, 2013.

Pelto, M. S., Miller, M. M., Adema, G. W., Beedle, M. J., McGee, S. R., Sprenke, K. F. and Lang, M.: The equilibrium flow and mass balance of the Taku Glacier, Alaska 1950–2006, The Cryosphere, 2(2), 147–157, doi:10.5194/tc-2-147-2008, 2008.

Pelto, M., Kavanaugh, J. and McNeil, C.: Juneau Icefield Mass Balance Program 1946–2011, Earth Syst. Sci. Data, 5(2), 319–330, doi:10.5194/essd-5-319-2013, 2013.

Pfeffer, W. T., Arendt, A. A., Bliss, A., Bolch, T., Cogley, J. G., Gardner, A. S., Hagen, J.-O., Hock, R., Kaser, G., Kienholz, C., Miles, E. S., Moholdt, G., Moelg, N., Paul, F., Radic, V., Rastner, P., Raup, B. H., Rich, J., Sharp, M. J., Andeassen, L. M., Bajracharya, S., Barrand, N. E., Beedle, M. J., Berthier, E., Bhambri, R., Brown, I., Burgess, D. O., Burgess, E. W., Cawkwell, F., Chinn, T., Copland, L., Cullen, N. J., Davies, B., De Angelis, H., Fountain, A. G., Frey, H., Giffen, B. A., Glasser, N. F., Gurney, S. D., Hagg, W., Hall, D. K., Haritashya, U. K., Hartmann, G., Herreid, S., Howat, I., Jiskoot, H., Khromova, T. E., Klein, A., Kohler, J., Konig, M., Kriegel, D., Kutuzov, S., Lavrentiev, I., Le Bris, R., Li, X., Manley, W. F., Mayer, C., Menounos, B., Mercer, A., Mool, P., Negrete, A., Nosenko, G., Nuth, C., Osmonov, A., Pettersson, R., Racoviteanu, A., Ranzi, R., Sarikaya, M. A., Schneider, C., Sigurdsson, O., Sirguey, P., Stokes, C. R., Wheate, R., Wolken, G. J., Wu, L. Z. and Wyatt, F. R.: The Randolph Glacier Inventory: a globally complete inventory of glaciers, Journal of Glaciology, 60(221), 537–552, doi:10.3189/2014JoG13J176, 2014.

Rignot, E., Echelmeyer, K. and Krabill, W.: Penetration depth of interferometric synthetic-aperture radar signals in snow and ice, Geophysical Research Letters, 28(18), 3501–3504, 2001.

Round, V., Leinss, S., Huss, M., Haemmig, C. and Hajnsek, I.: Surge dynamics and lake outbursts of Kyagar Glacier, Karakoram, The Cryosphere, 11(2), 723–739, doi:10.5194/tc-11-723-2017, 2017.

Shean, D. E., Alexandrov, O., Moratto, Z. M., Smith, B. E., Joughin, I. R., Porter, C. and Morin, P.: An automated, open-source pipeline for mass production of digital elevation models (DEMs) from very-high-resolution commercial stereo satellite imagery, ISPRS Journal of Photogrammetry and Remote Sensing, 116, 101–117, doi:10.1016/j.isprsjprs.2016.03.012, 2016.

Wang, D. and Kääb, A.: Modeling Glacier Elevation Change from DEM Time Series, Remote Sensing, 7(8), 10117, 2015.

WGMS: Fluctuations of Glaciers Database. World Glacier Monitoring Service, Zurich, Switzerland. DOI:10.5904/wgms-fog-2017-10, 2017.

Ziemen, F. A., Hock, R., Aschwanden, A., Khroulev, C., Kienholz, C., Melkonian, A. and Zhang, J.: Modeling the evolution of the Juneau Icefield between 1971 and 2100 using the Parallel Ice Sheet Model (PISM), Journal of Glaciology, 62(231), 199–214, doi:10.1017/jog.2016.13, 2016.

Supplement

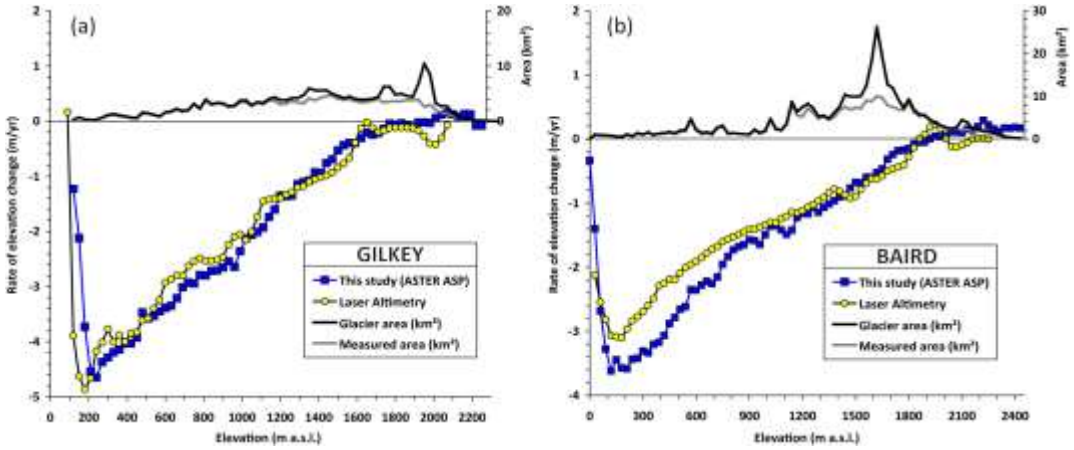

Supplementary Figure S1: Rates of elevation change vs. elevation for (a) Gilkey Glacier (Juneau Icefield) and (b) Baird Glacier (Stikine Icefield) measured from ASTER DEMs (blue curve, 2000-2016) and airborne laser altimetry data (2007-2012 for Gilkey and 1996-2013 for Stikine). The upper curve (right Y-axis) show the total area altitude distribution (black) and the glacier area effectively sampled using in the $ASTER_{dh/dt}$ (grey).

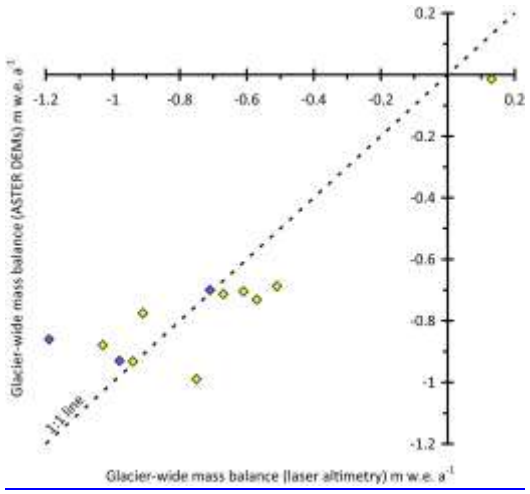

Supplementary Figure S2: Glacier-wide mass balances (Ba) of individual glaciers of the JIF (yellow, 9 glaciers) and SIF (blue, 3 glaciers) calculated in this study using ASTER DEMs from 2000 to 2016 and derived from airborne laser altimetry for different periods (Larsen et al., 2015). The dashed line is the 1:1 line.